Available at www.sciencedirect.com
ScienceDirect
journal homepage: www.elsevier.com/locate/carbon

Controllable seeding of single crystal graphene islands from graphene oxide flakes

Qiongyu Li [a], Cankun Zhang [a], Weiyi Lin [a], Zhiyi Huang [a], Lili Zhang [b], Hongyang Li [a], Xiangping Chen [a], Weiwei Cai [a], Rodney S. Ruoff [c,d,*], Shanshan Chen [a,*]

[a] Department of Physics, Laboratory of Nanoscale Condensed Matter Physics, Xiamen University, Xiamen 361005, China
[b] Heterogeneous Catalysis, Institute of Chemical Engineering and Sciences, Singapore 627833, Singapore
[c] Department of Mechanical Engineering and the Materials Science and Engineering Program, The University of Texas at Austin, Austin, TX 78712, USA
[d] IBS Center for Multidimensional Carbon Materials, Ulsan National Institute of Science and Technology (UNIST), Ulsan 689-798, Republic of Korea

ARTICLE INFO

Article history:
Received 3 May 2014
Accepted 30 July 2014
Available online 6 August 2014

ABSTRACT

Graphene oxide (G-O) flakes were used to seed the growth of single crystal graphene islands by chemical vapor deposition (CVD) on Cu foil. Such islands have the G-O seed (which converts to a 'reduced graphene oxide' (rG-O) seed due to the CVD growth conditions used) roughly in the center of the islands. The lateral growth of such single crystal graphene islands was studied by carbon isotope labeling and Raman spectroscopy, scanning and transmission electron microscopy and selected area electron diffraction. By changing the concentration of G-O in the aqueous dispersion used to deposit the G-O flakes onto the Cu foil by dip-coating, the size of the seeded graphene islands could be precisely controlled on the Cu foil. The crystal orientation of the single crystal graphene islands was found to be identical to that of the G-O seeds.

1. Introduction

CVD has been used to produce high quality monolayer and multilayer graphene films on various metal substrates [1–6]. For example, 30-inch diagonal monolayer graphene has been made by this relatively simple method [7]. CVD-grown graphene films are polycrystalline and thus have grain boundaries [8,9], which can degrade their physical and chemical properties [10–13]. It is therefore an important goal to synthesize large-scale, high-quality single crystal graphene to minimize the impact of grain boundaries. Control of the growth of graphene, especially during the initial stages of growth, is critical. A variety of growth parameters have been studied such as the type of carbon precursor, flow rate of methane [14], the effect of hydrogen partial pressure [15] and smoothness of the Cu foil surface before growth [16,17] in attempts to grow graphene with improved quality. However, the wide variation in grain size, shape, and film quality of graphene from lab-to-lab suggests there is room for improvement.

Seeding growth of CVD graphene using pre-patterned polymethyl methacrylate (PMMA) (prepared by E-beam lithography) or exfoliated graphene/graphite has been reported by Yu et al. [18,19]. Wang et al., reported "homoepitaxial" growth of graphene using exfoliated graphite flakes as seeds,

* *Corresponding authors:* Address: Department of Mechanical Engineering and the Materials Science and Engineering Program, The University of Texas at Austin, Austin, TX 78712, USA (R.S. Ruoff).
E-mail addresses: ruoffrs@gmail.com (R.S. Ruoff), sschen@xmu.edu.cn (S. Chen).
http://dx.doi.org/10.1016/j.carbon.2014.07.083
0008-6223/

however the graphene grown from the seeds was surrounded by graphene islands that nucleated independently of the seeds [20]. Teng et al., used exfoliated graphite flakes on SiO_2 substrates to seed the formation of graphene layers [21]. Wu et al., on the other hand, reported the growth of continuous graphene films at low temperatures down to 300 °C by introducing coronene as nucleation seeds [22]. Here, we demonstrate an effective approach to achieve single crystal graphene using G-O 'flakes' as seeds by CVD, and we explore some fundamental aspects of this type of seed-assisted growth. G-O flakes were chosen so as to obtain monolayer or few-layer graphene sheets. The graphene grown from the (reduced) G-O flake edges was studied by carbon isotope labeling and Raman mapping, as well as transmission electron microscopy (TEM) and selected area electron diffraction (SAED). It was found that the orientation of the graphene islands was identical to that of the G-O seeds. The density and size of the graphene islands could be controlled by adjusting the surface concentration of the G-O sheets and growth conditions. It was also possible to grow multilayer graphene from multilayer G-O seeds.

2. Results and discussion

G-O was dispersed in deionized water (0.05 mg/ml) by the sonication of graphite oxide powder, produced by the modified Hummers method [23,24]. G-O flakes were deposited on a Cu foil by dip-coating and drying, as shown in Fig. 1. In an attempt to remove any undesirable residue from the suspension that might act as unwanted nucleation sites during graphene growth, the Cu foil with the G-O flakes on it was rinsed in de-ionized water after annealing at 300 °C in hydrogen for 10 min. The annealing partially reduces the G-O flakes and prevents them from dislodging in de-ionized water. The Cu foil with the partially reduced G-O flakes (rG-O) was loaded into a quartz tube and growth was carried out at 1035 °C under 0.1 sccm $^{13}CH_4$ and 10 sccm H_2 for 20 min in the CVD system [25]. To explore whether the rG-O acted as seeds, $^{13}CH_4$ was used rather than normal methane [26], as described later. After growth, the graphene islands were transferred onto SiO_2/Si wafers and TEM grids by methods previously reported [27].

Atomic force microscopy (AFM) (SEIKO, SPA400) was used to evaluate the size distribution of G-O flakes deposited on the Cu foil or SiO_2/Si wafer pieces by dip-coating (Fig. 2a). Fig. 2c shows that the size distribution of the G-O flakes is close to a Gaussian distribution with an average lateral size of about 2.5 μm. Raman spectra of the G-O flakes shown in Fig. 2b exhibit two strong peaks at ~1350 and ~1600 cm^{-1}, corresponding to the D and G bands, respectively.

Micro-Raman mapping was used to map the ^{12}C vs ^{13}C regions of the isotope-labeled samples [28]. Raman mapping and spectroscopy (WITec Alpha-300, 488 nm excitation laser) was done after graphene growth on a Cu foil with rG-O flakes using a $^{13}CH_4$ precursor. The carbon film (i.e., islands) was transferred to a SiO_2/Si wafer. Fig. 3a and b show maps of the 2D peak (2550–2620 cm^{-1}) of ^{13}C graphene and the G_{12} peak (1550–1620 cm^{-1}) acquired from this growth run. A dark region is seen in the center of each island in the $2D_{13}$ map, and these same regions are bright in the G_{12} map, which proves that the rG-O flakes act as seeds for the lateral growth of ^{13}C graphene islands. Fig. 3d is a high resolution map of an island which is marked by the white dotted rectangle in Fig. 3b. The sizes of the rG-O seeds appear to be smaller after

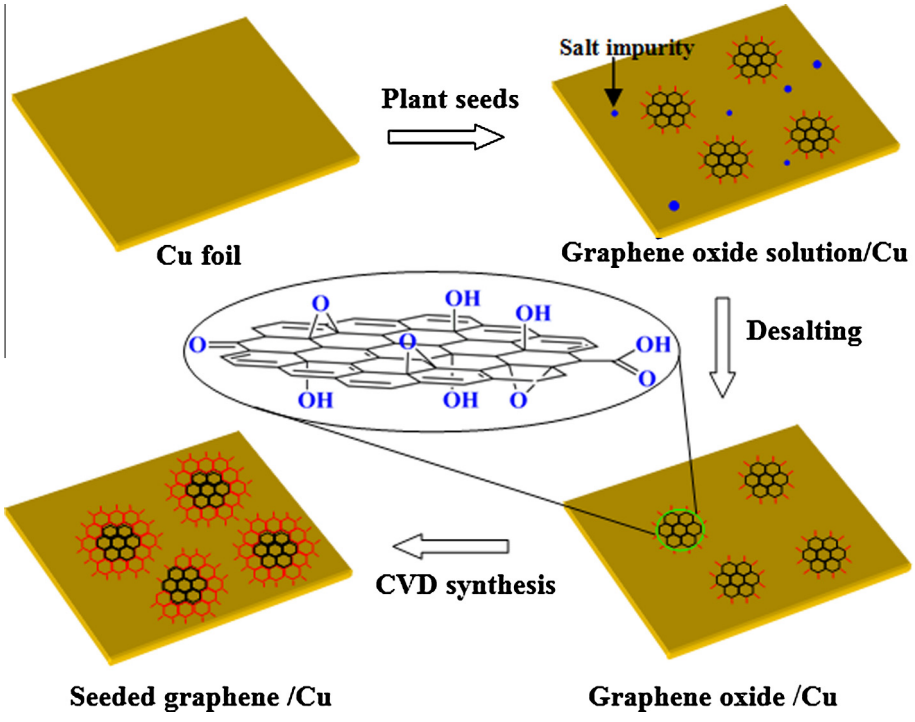

Fig. 1 – Illustration of the lateral growth by CVD of single crystal graphene islands on a Cu foil using G-O flakes as seeds. (A color version of this figure can be viewed online.)

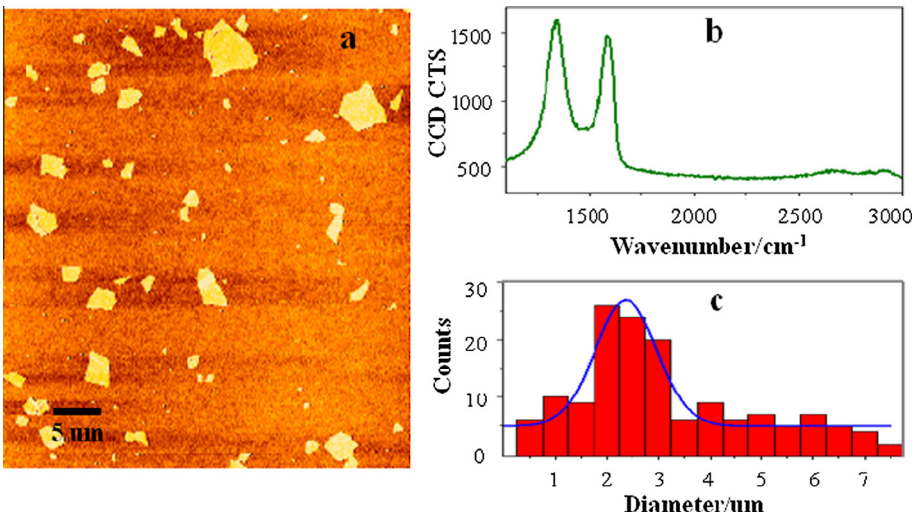

Fig. 2 – (a) AFM image and (b) Raman spectra of G-O flakes dip-coated on a SiO_2/Si wafer. (c) Histogram of the diameter distribution of G-O flakes. The solid line is a fit to the experimental data with a normal distribution. (A color version of this figure can be viewed online.)

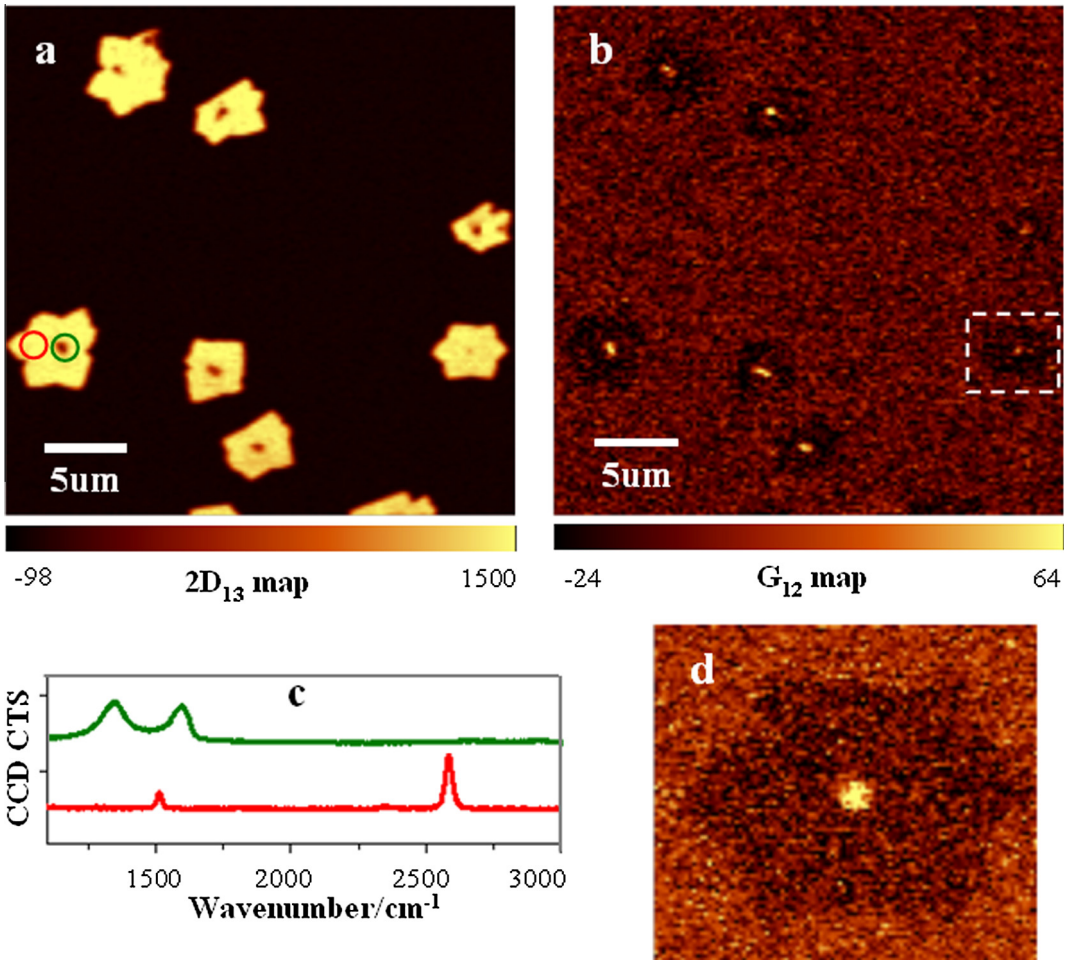

Fig. 3 – (a, b) Raman maps of $2D_{13}$ (2550–2620 cm^{-1}) and G_{12} (1550–1620 cm^{-1}) peaks of the G-O seeded graphene-island sample grown on a Cu foil then transferred onto a SiO_2/Si wafer. (c) Raman spectra taken from the green circle and the red circle in (a). (d) High resolution map of the island which is marked by the white dotted rectangle in (b). (A color version of this figure can be viewed online.)

growth (as estimated from Raman mapping) compared with the size before growth (as measured by AFM). It is possible that the rG-O was partially etched by hydrogen or other residual gases during the high temperature graphene CVD growth process [29–31]. Typical Raman spectra taken from the island center region (labeled by the green circle in Fig. 3a) show peaks from the rG-O seeds assigned as D_{12} (1350 cm^{-1}) and G_{12} (1600 cm^{-1}). The Raman spectrum taken from the region indicated by the red circle in Fig. 3a has sharp G_{13} and $2D_{13}$ peaks with a G/2D ratio less than 0.5 (Fig. 3c), which confirms that the graphene grown laterally from the rG-O seed is single-layer with no defect-related D peak detected.

The kinetics of the two-dimensional nucleation and growth of graphene on Cu surfaces has been both theoretically and experimentally investigated [32–37]. It is believed that the decomposition of methane leads to supersaturation of carbon adatoms at the Cu surface. In this model, the concentration of the active carbon species reaches a critical supersaturation point (C_{nuc}), then the nucleation of stable graphene nuclei takes place and the graphene islands begin

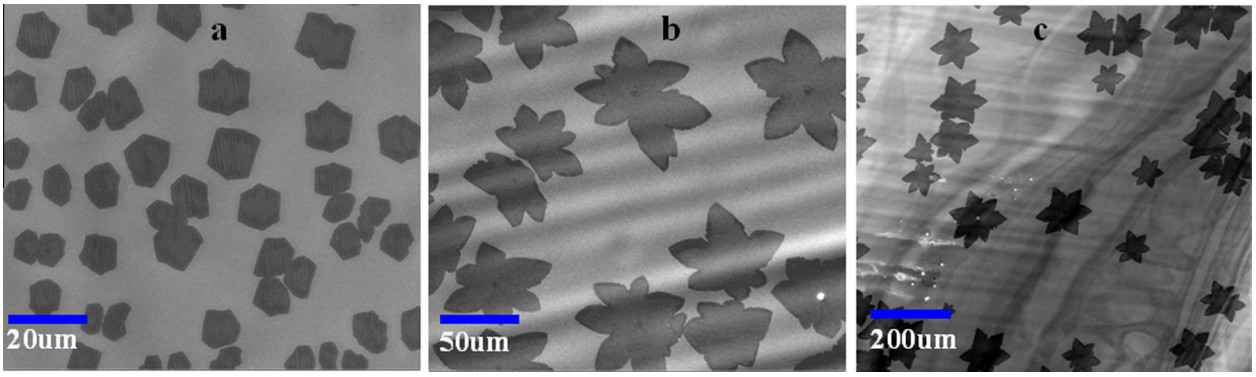

Fig. 4 – SEM images of G-O seeded graphene islands on a Cu foil arising from G-O concentrations of (a) 0.05 mg/ml, (b) 0.005 mg/ml and (c) 0.001 mg/ml used for the G-O deposition by dip-coating. (A color version of this figure can be viewed online.)

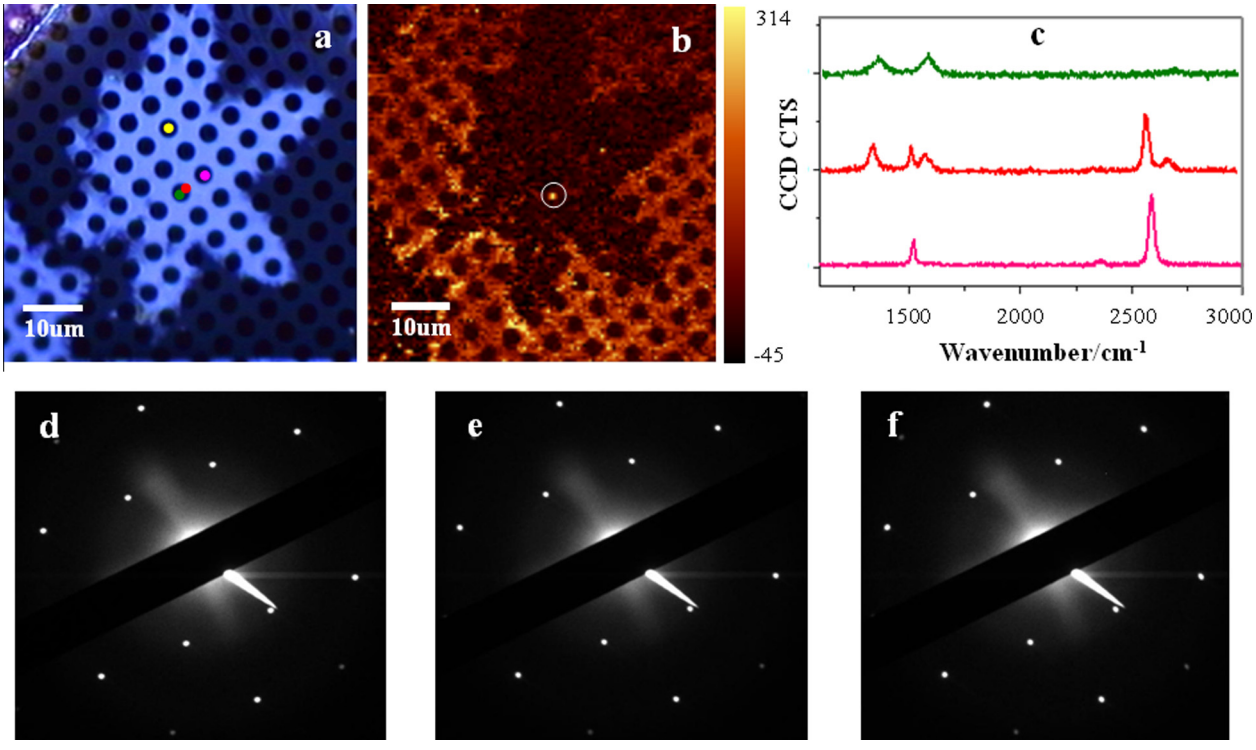

Fig. 5 – (a) Optical image of a seeded graphene island transferred onto a Quantifoil TEM grid after Raman mapping of that same island on the Quantifoil. (b) Raman D_{12} peak (1310–1390 cm^{-1}) map of the G-O seeded graphene island. (c) Raman spectra taken from different regions of the grown graphene. (d–f) TEM SAED of the same G-O seeded graphene island taken from (d) the center region with green spot, and (e, f) from the laterally grown graphene regions marked with pink and yellow spots. (A color version of this figure can be viewed online.)

to grow. As the growth proceeds, graphene islands either coalesce to eventually form a continuous film or stop growing to reach a saturated, final incomplete coverage. Here, we aimed to tune the graphene island density by adjusting the surface concentration of seeds by adjusting the concentration of the G-O dispersion. The growth conditions (temperature, flow, pressure, etc.) for all control samples were held the same, and adjusted so that the density of self-nucleation sites would be much lower than the seed density. Fig. 4 shows SEM images of three Cu foil samples that were dip-coated in 0.05, 0.005 and 0.001 mg/ml aqueous G-O dispersions (samples **S1**, **S2**, and **S3**, respectively) and annealed and washed with deionized water, before exposure to the same growth conditions (1035 °C under 0.1 sccm $^{13}CH_4$ and 10 sccm H_2 for 20 min). The graphene island density of sample **S1** is about 25 times higher than for sample **S2** and about 200 times higher than for sample **S3**, confirming that growth from the rG-O seeds plays the dominant role in graphene growth.

The graphene sample was transferred onto a Quantifoil® TEM grid and optical and Raman mapping images were made to help locate the seeds and graphene. Fig. 5a shows an optical image of a transferred isotope-labeled rG-O seeded graphene island, with the D_{12} peak (1310–1390 cm^{-1}) Raman map of the same area shown in Fig. 5b. The bright spot (indicated by the white circle in Fig. 5b) in the center of the island is confirmed by its characteristic Raman spectrum (Fig. 5c) to be the rG-O seed (that is, what was originally the G-O flake) and the size of the seed is estimated to be ~2 μm. A complete survey of this particular transferred graphene island was done by TEM (JEM-2010F), by obtaining SAED data from different regions of the island including the 'seed' region. Typical results, Fig. 5d–f, show that the SAED patterns taken from the green, pink and yellow 'regions' in Fig. 5a have identical SAED patterns. This shows that the graphene that grows laterally from the rG-O seed has the same crystal orientation.

Although the seeded graphene islands are mostly monolayer, some multilayer graphene islands were also obtained. Fig. 6a shows an optical image of a seeded multilayer graphene island after transfer to a SiO_2/Si wafer. The changes in contrast indicate that the film is not uniform in thickness and consists of approximately three layers (enlarged in the inset of Fig. 6a). Fig. 6b shows the Raman spectra taken from the different spots on the multilayer graphene island shown in Fig. 6d. Raman maps of the D_{12} peak (1350–1420 cm^{-1})

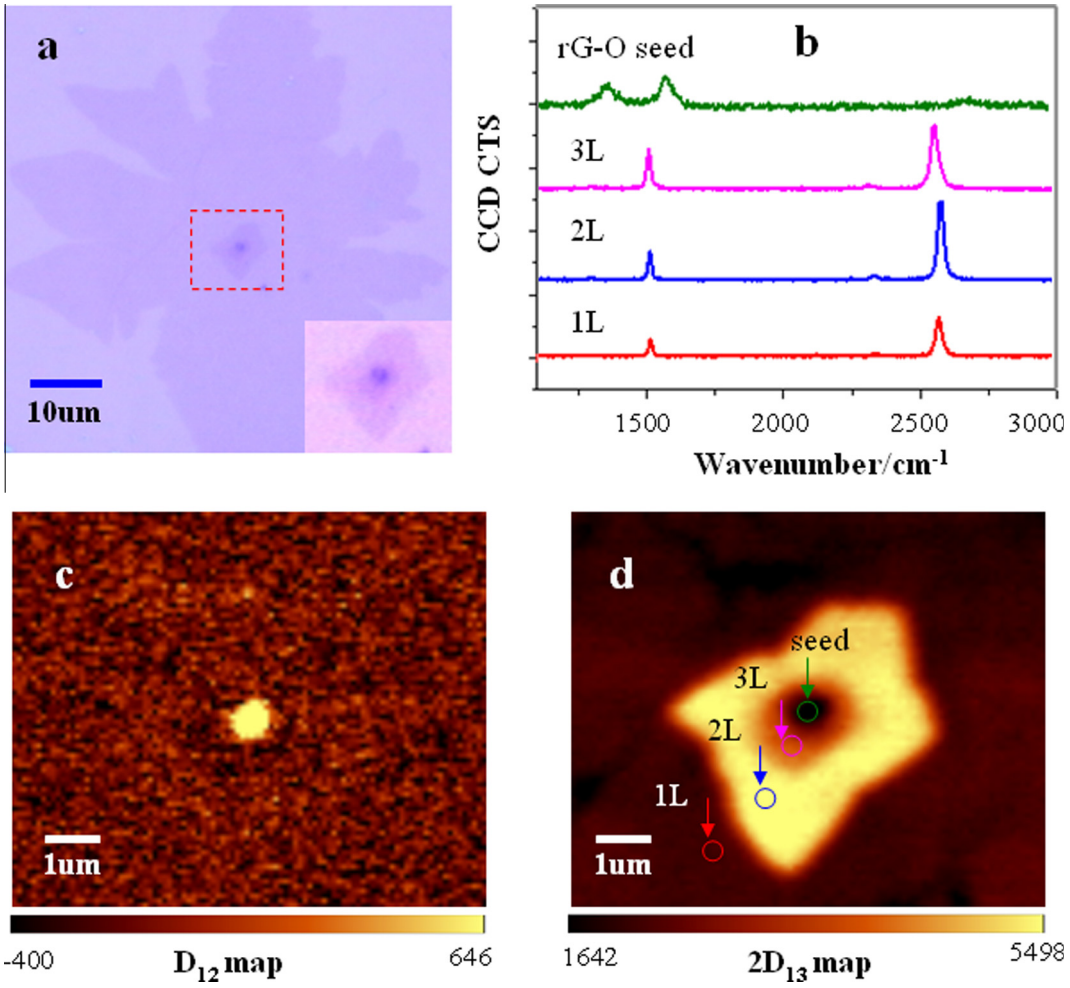

Fig. 6 – (a) Optical image of a seeded multilayer graphene island transferred onto a SiO_2/Si wafer. (b) Raman spectra taken from different spots from the laterally grown multilayer graphene region shown in (d). (c, d) D_{12} (1350–1420 cm^{-1}) and $2D_{13}$ (2550–2620 cm^{-1}) Raman maps of the rectangular region in (a). (A color version of this figure can be viewed online.)

and $2D_{13}$ peak (2550–2620 cm^{-1}) of the multilayer region marked by the red dotted rectangle in Fig. 6a clearly map the seed region (from D_{12} peak mapping in Fig. 6c) and the grown graphene layers (from $2D_{13}$ peak mapping in Fig. 6d). We found that a large fraction of the seeded multilayer graphene does not have AB stacking. We suggest this is possibly due to multilayer G-O flakes acting as the seed of these multilayer graphene islands, and the possibility that these are also not AB-stacked.

3. Conclusion

Control of the growth of CVD graphene on Cu foil was achieved by using G-O (converted to rG-O) flakes as seeds. Micro-Raman spectroscopy and mapping and TEM with SAED show these flakes served as seeds for the growth of single layer or multilayer graphene from their edges, and that the single layer graphene islands are single crystal and of the same crystal orientation as the rG-O flakes. The size of the single crystal graphene can be controlled by adjusting the areal density of the seeds.

4. Experimental section

4.1. *Preparation of G-O dispersion in water*

Graphite oxide was prepared from natural graphite powder (Bay Carbon, SP-1 graphite) using the 'modified Hummers method' [24]. Briefly, the graphite powder was oxidized to graphite oxide using H_2SO_4 and $KMnO_4$ (Sigma Aldrich). The mixture was centrifuged after filtration while warm and washed with warm DI water (resistivity about 1 MΩ cm). Aqueous dispersions of graphene oxide (G-O) were then prepared by transferring a given weight of the graphite oxide to the deionized water, and dispersing by sonication.

4.2. *Transfer of seeded graphene*

The as-grown graphene film (always sub-monolayer coverage with graphene islands separated by bare Cu) on the Cu foil was spin-coated with PMMA (average M_w ~996,000 by GPC, Sigma–Aldrich product No. 182265, dissolved in chlorobenzene with a concentration of 46 mg/mL). The Cu foil was then etched away by an aqueous solution of ammonium persulfate (0.03 g/mL, Sigma Aldrich)) over a period of 12 h. The PMMA-coated graphene was washed with deionized water and placed on the target substrates. The whole sample was dried in vacuum, which gave a good contact between graphene and the substrate. The PMMA was then dissolved using acetone so that the film (i.e., graphene islands) remained on the target substrates.

4.3. *Characterization*

SEM images were taken with an FEI Quanta-600 FEG Environmental SEM using an acceleration voltage of 30 kV. Raman spectra (WITec Alpha-300) were obtained with a 488 nm laser (~10 mW power) source.

Acknowledgements

This work was supported by the National Natural Science Foundation of China (Nos. 51302233, 11374244 and 11335006), and the Specialized Research Fund of the Doctoral Program of Higher Education (SRFDP, 20130121120017). RSR appreciates support from the Institute of Basic Science, Center for Multidimensional Carbon Materials.

REFERENCES

[1] Li XS, Cai WW, An J, Kim S, Nah J, Yang DX, et al. Large-area synthesis of high-quality and uniform graphene films on copper foils. Science 2009;324(5932):1312–4.
[2] Kim KS, Zhao Y, Jang H, Lee SY, Kim JM, Kim KS, et al. Large-scale pattern growth of graphene films for stretchable transparent electrodes. Nature 2009;457(7230):706–10.
[3] Li XS, Cai WW, Colombo L, Ruoff RS. Evolution of graphene growth on Ni and Cu by carbon isotope labeling. Nano Lett 2009;9(12):4268–72.
[4] Chen SS, Cai WW, Piner RD, Suk JW, Wu YP, Ren YJ, et al. Synthesis and characterization of large-area graphene and graphite films on commercial Cu–Ni alloy foils. Nano Lett 2011;11(9):3519–25.
[5] Marchini S, Günther S, Wintterlin J. Scanning tunneling microscopy of graphene on Ru(0001). Phys Rev B 2007;76(7):075421.
[6] Reina A, Jia XT, Ho J, Nezich D, Son HB, Bulovic V, et al. Layer area, few-layer graphene films on arbitrary substrates by chemical vapor deposition. Nano Lett 2009;9(8):3087–8.
[7] Bae S, Kim H, Lee Y, Xu XF, Park JS, Zheng Y, et al. Roll-to-roll production of 30-inch graphene films for transparent electrodes. Nat Nanotechnol 2010;5(8):574–8.
[8] Chen SS, Brown L, Levendorf M, Cai WW, Ju SY, Edgeworth J, et al. Oxidation resistance of graphene-coated Cu and Cu–Ni alloy. ACS Nano 2011;5(2):1321–7.
[9] Wofford JM, Nie S, McCarty KF, Bartelt NC, Dubon OD. Graphene islands on Cu foils: the interplay between shape, orientation, and defects. Nano Lett 2010;10(12):4890–6.
[10] Grantab R, Shenoy VB, Ruoff RS. Anomalous strength characteristics of tilt grain boundaries in graphene. Science 2010;330(6006):946–8.
[11] Haque MA, Saif MT. Deformation mechanisms in free-standing nanoscale thin films: a quantitative in situ transmission electron microscope study. Proc Natl Acad Sci U S A 2004;101(17):6335–40.
[12] Lei QF, Lin RS, Ni DY, Hou YC. Thermal conductivities of some organic solvents and their binary mixtures. J Chem Eng Data 1997;42(5):971–4.
[13] Bagri A, Kim SP, Ruoff RS, Shenoy VB. Thermal transport across twin grain boundaries in polycrystalline graphene from nonequilibrium molecular dynamics simulations. Nano Lett 2011;11(9):3917–21.
[14] Bhaviripudi S, Jia X, Dresselhaus MS, Kong J. Role of kinetic factors in chemical vapor deposition synthesis of uniform large area graphene using copper catalyst. Nano Lett 2010;10(10):4128–33.
[15] Vlassiouk I, Regmi M, Fulvio MP, Dai S, Datskos P, Eres G, et al. Role of hydrogen in chemical vapor deposition growth of large single-crystal graphene. ACS Nano 2011;5(7):6069–76.
[16] Yan Z, Lin J, Peng ZW, Sun ZZ, Zhu Y, Li L, et al. Toward the synthesis of wafer-scale single-crystal graphene on copper foils. ACS Nano 2012;6(10):9110–7.

[17] Wang H, Wang G, Bao P, Yang S, Zhu W, Xie X, et al. Controllable synthesis of submillimeter single-crystal monolayer graphene domains on copper foils by suppressing nucleation. J Am Chem Soc 2012;134(8):3627–30.
[18] Yu QK, Jauregui LA, Wu W, Colby R, Tian JF, Su ZH, et al. Control and characterization of individual grains and grain boundaries in graphene grown by chemical vapour deposition. Nat Mater 2011;10(6):443–9.
[19] Wu W, Jauregui LA, Su Z, Liu Z, Bao J, Chen YP, et al. Growth of single crystal graphene arrays by locally controlling nucleation on polycrystalline Cu using chemical vapor deposition. Adv Mater 2011;23(42):4898–903.
[20] Wang H, Wang GZ, Bao PF, Shao ZB, Zhang X, Yang SL, et al. Lateral homoepitaxial growth of graphene. CrystEngComm 2014;16(13):2593–7.
[21] Teng PY, Lu CC, Akiyama-Hasegawa K, Lin YC, Yeh CH, Suenaga K, et al. Remote catalyzation for direct formation of graphene layers on oxides. Nano Lett 2012;12(3):1379–84.
[22] Wu T, Ding G, Shen H, Wang H, Sun L, Zhu Y, et al. Continuous graphene films synthesized at low temperatures by introducing coronene as nucleation seeds. Nanoscale 2013;5(12):5456–61.
[23] Cote LJ, Kim F, Huang J. Langmuir–Blodgett assembly of graphite oxide single layers. J Am Chem Soc 2009;131(3):1043–9.
[24] Hummers WS, Offeman RE. Preparation of graphitic oxide. J Am Chem Soc 1958;80(6):1339.
[25] Chen SS, Ji HX, Chou H, Li QY, Li HY, Suk JW, et al. Millimeter-size single-crystal graphene by suppressing evaporative loss of Cu during low pressure chemical vapor deposition. Adv Mater 2013;25(14):2062–5.
[26] Li Q, Chou H, Zhong JH, Liu JY, Dolocan A, Zhang J, et al. Growth of adlayer graphene on Cu studied by carbon isotope labeling. Nano Lett 2013;13(2):486–90.
[27] Li XS, Zhu YW, Cai WW, Borysiak M, Han BY, Chen D, et al. Transfer of large-area graphene films for high-performance transparent conductive electrodes. Nano Lett 2009;9(12):4359–63.
[28] Chen SS, Wu QZ, Mishra C, Kang JY, Zhang HJ, Cho K, et al. Thermal conductivity of isotopically modified graphene. Nat Mater 2012;11(3):203–7.
[29] Zhang Y, Li Z, Kim P, Zhang LY, Zhou CW. Anisotropic hydrogen etching of chemical vapor deposited graphene. ACS Nano 2012;6(1):126–32.
[30] Zhang XF, Ning J, Li XL, Wang B, Hao L, Liang MH, et al. Hydrogen-induced effects on the CVD growth of high-quality graphene structures. Nanoscale 2013;5(18):8363–6.
[31] Wang B, Zhang YH, Zhang HR, Chen ZY, Xie XM, Sui YP, et al. Wrinkle-dependent hydrogen etching of chemical vapor deposition-grown graphene domains. Carbon 2014;70:75–80.
[32] Johnson WA, Mehl RF. Reaction kinetics in processes of nucleation and growth. Trans Am Inst Min Metall Pet Eng 1939;135(8):396–415.
[33] Kim H, Mattevi C, Calvo MR, Oberg JC, Artiglia L, Agnoli S, et al. Activation energy paths for graphene nucleation and growth on Cu. ACS Nano 2012;6(4):3614–23.
[34] Loginova E, Bartelt NC, Feibelman PJ, McCarty KF. Evidence for graphene growth by C cluster attachment. New J Phys 2008;10(9):093026.
[35] Van Wesep RG, Chen H, Zhu W, Zhang Z. Communication: stable carbon nanoarches in the initial stages of epitaxial growth of graphene on Cu(111). J Chem Phys 2011;134(17):171105.
[36] Loginova E, Bartelt NC, Feibelman PJ, McCarty KF. Factors influencing graphene growth on metal surfaces. New J Phys 2009;11(6):063046.
[37] Zhang WH, Wu P, Li ZY, Yang JL. First-principles thermodynamics of graphene growth on Cu surfaces. J Phys Chem C 2011;115(36):17782–7.